EARTHQUAKE ENGINEERING AND STRUCTURAL DYNAMICS
Earthquake Engng Struct. Dyn. 2001; **30**:1061–1081 (DOI: 10.1002/eqe.52)

Evaluation of the seismic response of masonry buildings based on energy functions

D. Benedetti[1,*,†], P. Carydis[2] and M. P. Limongelli[1]

[1]*Department of Structural Engineering, Politecnico di Milano, Milan, Italy*
[2]*Laboratory of Earthquake Engineering, National Technical University of Athens, Athens, Greece*

SUMMARY

This work is based on energies evaluated from the responses of 12 stone and brick masonry systems subjected to 58 shaking table tests. The evolution of input energy during a damaging base excitation is correlated to the change of the damage patterns of the considered buildings. The comparison among energies dissipated and absorbed by the buildings during the various shocks gives some hints on strengthening strategies. It is found that damage to spandrel beams produces a more significant energy absorption than other types of damage. Copyright © 2001 John Wiley & Sons, Ltd.

KEY WORDS: energy functions; damage index; masonry buildings; strengthening

1. INTRODUCTION

A few years ago a large number of shaking table tests on masonry buildings were carried out in the realm of an experimental research funded by the European Commission (CEC). The aim of the research, whose main results can be found in Reference [1], was to analyse the efficiency of various retrofitting techniques in improving the seismic behaviour of non-engineered masonry buildings. Buildings were scaled 1 : 2 and were of two types: stone and brick masonry, respectively denoted in the following as SM and BM. The latter were tested in their original configurations up to medium–severe damage and then repaired and again tested. Stone masonry systems were strengthened prior to tests. The only stone masonry building tested in its original configuration collapsed due to wall separation. Buildings were excited by three-component base motions of similar peak acceleration and were subjected to excitations of increasing severity, starting from very low values of accelerations. The number of three-component shocks acting on each building ranged from 3 to 7. Two types of signals were

* Correspondence to: D. Benedetti, Department of Structural Engineering, Politecnico di Milano, Piazza Leonardo da Vinci 32, I-20133 Milan, Italy.
† E-mail: dbened@stru.polimi.it

Received 8 February 2000
Revised 25 May 2000 and 13 September 2000
Accepted 24 October 2000

Table I. Tested buildings.[†]

Building	Mat.	Repair/ strengthening	a_M (g units)	Input	No. of shocks
A1	BM	sc	0.32	S	5
A2	BM	lsc-rb-sn2	0.43	S	6
B1	BM	—	0.33	L	5
B2	BM	lsc-sn1,2	0.42	L	5
C1	BM	—	0.26 (0.27)	L	4
C2	BM	lsc-ht-sn1,2	0.44	L	5
D1	BM	sc	0.30	S	5
D2	BM	lsc-ht	0.32	S	7
E1	SM	sc-rb	0.23 (0.24)	S	5
F1	SM	sn1,2	0.16 (0.17)	S	4
G1	SM	—	0.17 (0.19)	S	4
	SM	sc-ht	0.16	S	3

[†](BM) brick masonry, (SM) roughly squared stone masonry, (sc) steel connectors, (lsc) local sealing using cement mixture, (sni) steel network on slabs (i denotes the storey level), (rb) reinforced concrete band, (ht) horizontal tendons.

used: one about 80 sec long and the other 40 sec long. The second signal set was derived from the first one; both show basically the same frequency content (see Reference [1]). Table I lists the main characteristics of the buildings and of the relevant test sequences; Figure 1 shows schematically the configuration of the buildings.

In the table, S denotes the short signal and L the long one, a_M is the peak acceleration in g units of the last shock of the sequence. In some cases the last test was interrupted due to very heavy damage and the danger of a partial or total collapse. The latter occurred for building G1. The values of peak accelerations of interrupted shocks are reported between parentheses. Response accelerations were recorded at 18 locations during all 58 events. Both in Reference [1] and in what follows, all results and comments are referred to the real (modelled) building.

Based on these records absolute energies, according to the definition given in Reference [2], have been computed and correlated to the observed damage. This was made for the entire set of shocks. For each of them and for each building the variation with time of the cumulated input energy $e_{Ij}(t)$, where the index j refers to the jth shock acting on the given building, has been computed. Additionally, each base time history has been described by a 'referential energy' $r_j(t)$, defined below. Based on these functions a 'performance index' $i_j(t)$ was introduced. The variations with time of $e_{Ij}(t)$ and $i_j(t)$ are compared to the variations of the effective stiffness of the dominant mode along the considered direction. The values of the above three functions, when computed at the end of each shock, describe, respectively, the total hysteretic and damping energy, the total 'referential energy' of the shock and the total 'performance' index for the given building and the given base excitation. These quantities, compared to the damage pattern detected during the relevant shock, allow description of the global behaviour of each building during the entire set of shocks that acted on it and comparison of the behaviours of buildings of different types and the effects of different strengthening and repairs. These comparisons gave some hints for establishing new technical interventions on existing buildings to enhance their energy dissipation and absorption capacity. Moreover, the analysis of the evolution during a single shock of the energy functions derived in the next section, allows

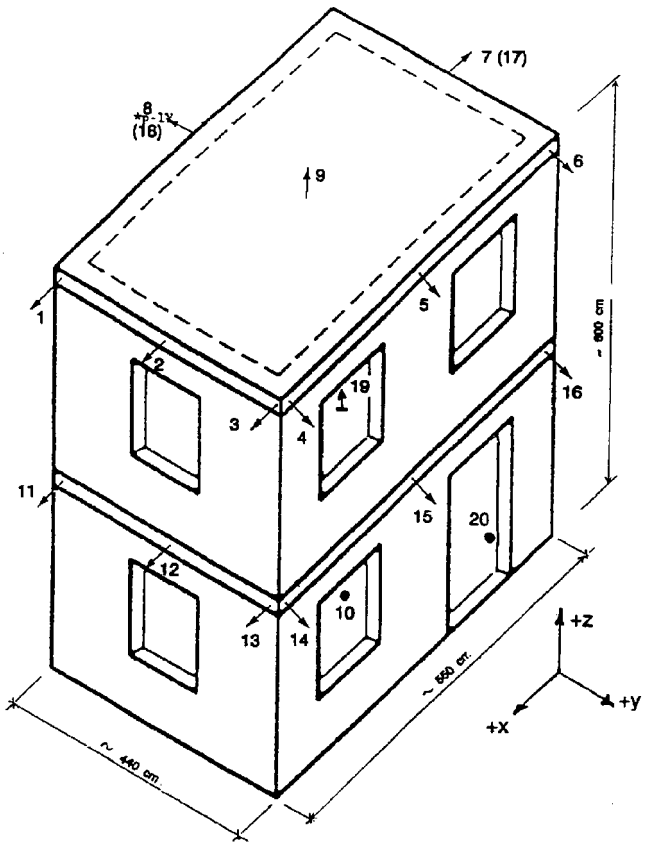

Figure 1. Scheme of the tested buildings (real sizes).

detection of the occurrence of damage, even when it is not fully visible. The use of these functions gives a method for the interpretation of the responses recorded during shaking table tests.

2. ENERGY FUNCTIONS INVOLVED

2.1. Input, damping and absorbed energies

Horizontal response accelerations are available, for each test, at 8 locations in the x direction, at 8 locations in the y direction and at 2 locations in the z direction, x and y being the principal plan directions and z the vertical one (see Figure 1). In principle, the dynamic behaviour of the building may be studied by associating a pertinent mass m_i to each location, thus looking at the real distributed mass system as a lumped mass one. For instance, by calling $\mathbf{u}(t)$ and $\mathbf{u}_t(t)$ the vectors of the relative and absolute displacements in the x direction at the said locations

the following classical equation holds:

$$\mathbf{m}\ddot{\mathbf{u}}_t + \mathbf{f}_\xi + \mathbf{f}_S = \mathbf{0} \tag{1}$$

where $\mathbf{f}_S$ is the restoring force vector, $\mathbf{f}_\xi$ is the viscous damping force vector and $\mathbf{m}$ the mass matrix. A similar equation may be written in the y direction. By integrating Equation (1) with respect to $\mathbf{u}$ the following energy equation in the x direction, at time t, is obtained (see Reference [2]):

$$e_{\mathrm{K}x}(t) + e_{\xi x}(t) + e_{\mathrm{A}x}(t) = e_{\mathrm{I}x}(t) \tag{2}$$

with $e_{\mathrm{K}x}(t)$ being the kinetic energy, $e_{\xi x}(t)$ the damping energy, $e_{\mathrm{A}x}(t)$ the absorbed energy and $e_{\mathrm{I}x}(t)$ the input energy. The absorbed energy may be split into two parts:

$$e_{\mathrm{A}x}(t) = e_{\mathrm{H}x}(t) + e_{\mathrm{S}x}(t) \tag{3}$$

with $e_{\mathrm{H}x}(t)$ being the hysteretic energy and $e_{\mathrm{S}x}(t)$ the strain energy. Quantities appearing in Equations (2) and (3) account for the responses in the x direction, which are also determined by the base input acting along the orthogonal direction y. Owing to the orthogonality of inertia forces and responses in the two considered directions, the total energy equation may be written as

$$(e_{\mathrm{K}x} + e_{\mathrm{K}y}) + (e_{\xi x} + e_{\xi y}) + (e_{\mathrm{A}x} + e_{\mathrm{A}y}) = (e_{\mathrm{I}x} + e_{\mathrm{I}y}) \tag{4}$$

In order to be able to derive analytically any of the above equations we should know the mechanical and dynamic properties of the system and the way they change during a given response. But we do not have this information, unless we refer to drastic simplifications and assumptions of uncertain reliability. However, based on measured responses one can compute $e_{\mathrm{I}}(t)$ and $e_{\mathrm{K}}(t)$ and hence may know the absorbed and damping energies $e_{\mathrm{A}}(t)$ and $e_{\xi}(t)$, in spite of being unable to distinguish the contributions of the different effects involved (elastic, damping and hysteretic phenomena). At the end of the ground shaking ($t = T$, T being its duration) Equations (2) and (3) become

$$e_{\xi x}(T) + e_{\mathrm{H}x}(T) = e_{\mathrm{I}x}(T), \text{ being } e_{\mathrm{K}x}(T) = e_{\mathrm{S}x}(T) = 0 \tag{5}$$

In what follows, quantities that refer to the end of the responses will be denoted by capital letters ($E_{\mathrm{I}}, E_{\xi}, E_{\mathrm{H}}$); they express the total input, damping and hysteretic energies during the given shock: at its end $E_{\mathrm{I}} = E_{\xi} + E_{\mathrm{H}}$.

2.2. Examples

As examples of some properties of the above functions, consider Figures 2(a) and 2(b) that show the evolution of the input energy (e_{I}) and of the absorbed and damping energies ($e_{\mathrm{A}} + e_{\xi}$), evaluated from the responses in the x direction for two shocks acting on the building A1 (brick masonry, originally undamaged). The two considered shocks are, respectively, the first and the last one of the testing sequence for A1. The first excitations are quite modest; peak accelerations of the three components of ground motion are of the order of $0.05g$, while the

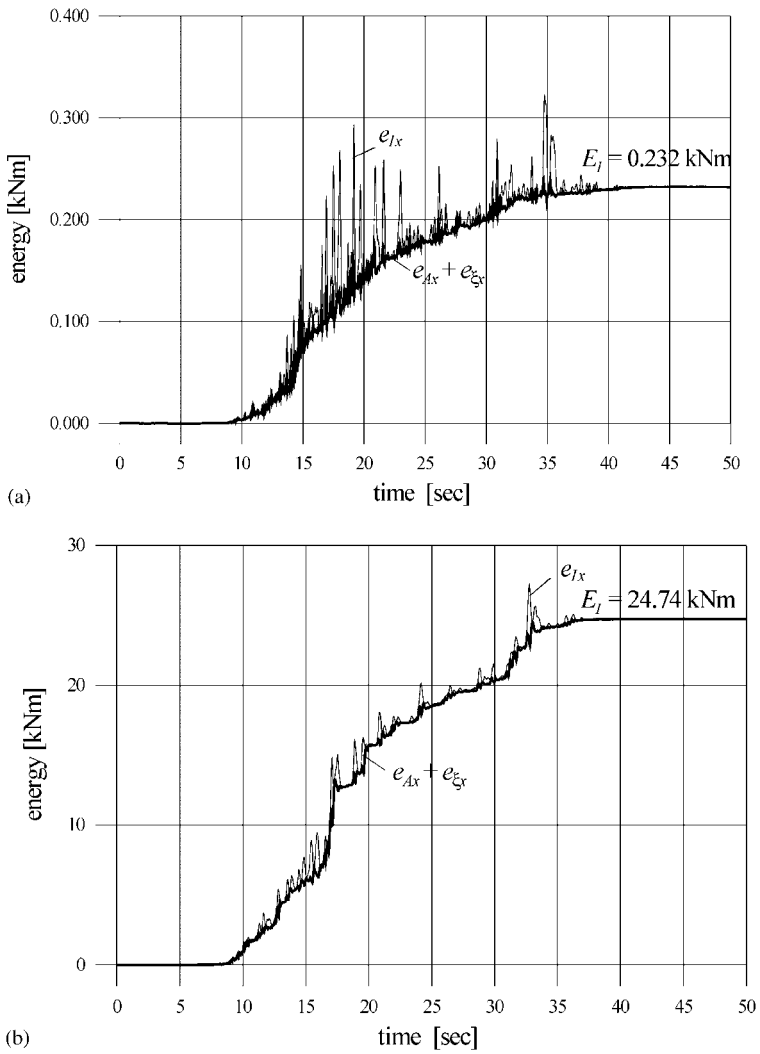

Figure 2. Energies evaluated from the responses in the x-direction for (a) the first test ($a_M \cong 0.05g$) on building A1, and (b) the last test ($a_M \cong 0.32g$) on building A1.

last excitations are rather severe (PGA of the order of $0.32g$). During the first test the structure suffered very slight damage at spandrel beams and behaved basically linearly; during the last test the building showed heavy damage at piers and at spandrel beams of both storeys. In the two figures $e_I(t)$ is more jagged than $(e_A + e_\xi)$ due to the contribution of the kinetic energy to e_I. This contribution is much more important during the first test than during the last one, when the heavy damage suffered by the building makes damping and hysteretic energies predominant with respect to e_K. If the kinetic energy e_K is subtracted from e_I, the function

$(e_A + e_\xi)$ is obtained. This function shows a similar jaggedness because of the contribution of the strain energy e_S to e_A. This contribution is more significant during the first test (Figure 2(a)) than during the last one (Figure 2(b)), due to the intact elastic properties of the building, which progressively deteriorate at the increase of damage.

During the last shock the function $(e_A + e_\xi)$ shows some steep increases, for instance at $t \cong 12, 16, 19$ sec, which do not occur during the first test. They point out an increase of damping and hysteretic energies, connected with the occurrence of new damage or with the extension of the existing one. This feature will be further commented on in the next section. The values of e_I are quite different in the two cases, with those during the last test being about 105 times higher than those of the first test. At the end of the two events E_I is, respectively, 0.232 and 24.74 kN m. Note that base inputs used in the two tests differ only in the values of accelerations, having been obtained by scaling with a constant factor the same reference signal: base accelerations of the last test are 6.4 times higher than the ones of the first test, but their frequency content is fairly similar. In the case of an ideal linear behaviour, with the same dynamic properties of the original building, during the last shock one would expect energies 41 times higher than those of the first test. Actual values are about double that, as can be seen from Figures 2(a) and 2(b), thus pointing out the considerable influence of damage on energy absorption and dissipation.

2.3. *Referential energy*

The comparison among the values of energies related to different severities of the base excitation is meaningful, as will be seen later. However, in some instances it is useful to normalize cumulated energy time histories with respect to the 'importance' of the excitation. For this purpose the following function is introduced, for each component of the ground motion:

$$r(t) = M \int_0^t |\ddot{u}_g \dot{u}_g| \, dt \tag{6}$$

M being the total mass of the building and $u_g(t)$ the ground displacement acting along the considered direction. This function will be referred to as 'referential energy': it is used only as a normalizing function and does not have a physical background if referred to real earthquakes. However, it may be seen as the work that would be done by the actuators of the table to produce the given motion $u_g(t)$, if the building were a rigid body of mass M. Hence it describes, although it does not measure, the energy made available to the building by the base motion $u_g(t)$. The total referential energy, at the end of the excitation, is denoted by R_x, R_y or $R = R_x + R_y$ depending on the direction taken into account. Figures 3(a) and 3(b) report $r(t)$, referred to the x-direction, for the building A1 and for the same shocks previously cited. It may be seen that these functions are more regular than $e_I(t)$ and $(e_A(t) + e_\xi(t))$ in the same direction and that they do not show steep increases like those of Figure 2(b). The evolution with time of $r(t)$ is directly connected with the evolution of the base input: as an example in both the considered tests the main part of the base acceleration time history (not shown here) occurs between 15 and 20 sec and this is reflected in the correspondent increase of $r(t)$ in the same time interval (see Figures 3(a) and 3(b)). The final values R for the two tests are quite different from each other, the one of the last shock being about 25 times larger than the one of the first test.

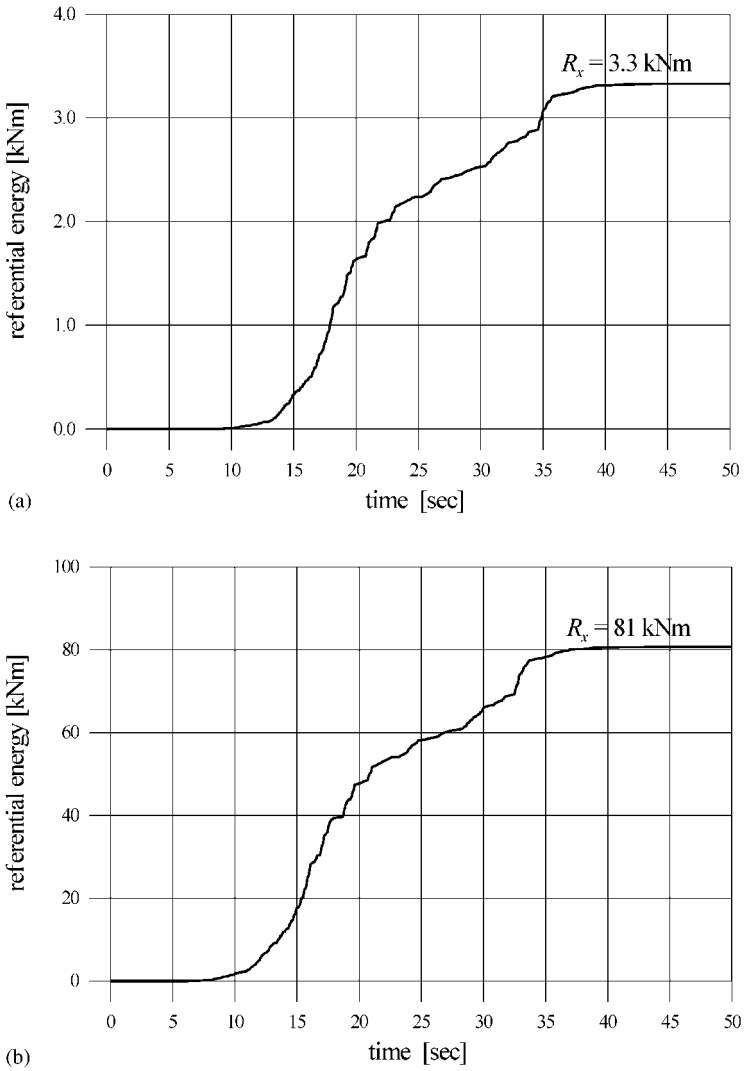

Figure 3. Referential energy in the x-direction for (a) the first shock on building A1 and (b) the last shock on building A1.

2.4. *Performance index*

For a better description of the behaviour of a building during a given excitation and in order to allow a comparison of the structural behaviour determined by shocks of different severity (which affect the values of all the above functions and parameters), the input energy $e_I(t)$ is normalized to $r(t)$ of the relevant shock and the following function is introduced:

$$i(t) = \frac{e_I(t)}{r(t)}$$

$i(t)$ is called 'performance index' and is related to the same direction which $e_I(t)$ and $r(t)$ are referred to. Its final value I may be considered as a description of the portion of the 'referential energy' provided by the base motion that has been dissipated and absorbed by the building during its response in the considered direction. This meaning also holds for $i(t)$ at any t value. For the two tests considered up to now, I is, respectively, 0.069 and 0.305. The very low value for the first test is related to the total energy dissipated through viscous damping, while the higher value for the last test accounts for the important hysteretic behaviour induced by the heavy damage suffered by the structure, which caused about 30 per cent of the 'referential energy' to be dissipated and absorbed by the building. Given its definition, the index is independent of the duration of the base motion, thus allowing to compare the structural behaviour of systems subjected to earthquakes of different durations. Increasing values of I and of $i(t)$ denote increasing damage and enhanced energy absorption and dissipation. In the ideal case of a linear undamped system, $I_x = I_y = I_t = 0$. One SM building collapsed during the last test (system G1) and the table was immediately stopped. From the available (interrupted) signals, the value $I_t = 0.61$ was obtained.

3. EVOLUTION DURING A GIVEN EARTHQUAKE

3.1. *Examples of time histories of e_I, i and k_{eff}*

In all tested buildings major damage occurred in x-walls (with windows at both storeys and doors at the first one). For this reason reference is made here to energy and index time histories evaluated from the signals recorded along the x-direction, although these functions have been determined also along the orthogonal y-direction. In the following energy notations the suffix x is dropped. In order to clarify the main items that characterize the response in terms of the above functions, in this section reference is made to systems A1 and C1. Figures 4(a) and 4(b) show, respectively, for the first and last shocks on A1, the functions $(e_A + e_\xi)$, $i(t)$, $r(t)$ and the effective stiffness k_{eff} of the first mode, which turned out to be predominant during the response.

The effective stiffness k_{eff} is defined (see Reference [1]) as the ratio of the restoring forces per unit mass to the relative displacements pertaining to the first mode. It is computed by band-pass filtering responses at a given location, around the modal frequency, previously determined through system identification. Modal restoring forces and displacements are correlated by quasi-elliptic cycles: the slope of their major axes determines the effective stiffness at the time corresponding to the maximum cycle displacement. In the case of perfectly linear response, the slope of the cycles is unchanged during the response. When the structure deteriorates, cycles widen and their slope decreases. The analysis of the evolution of k_{eff} during the base motion allows to detect the occurrence of damage, marked by a decrease of k_{eff}.

3.2. *Some properties of e_I, i and k_{eff}*

In Figures 4(a) and 4(b), cumulative energy functions are normalized to their peak values in order to facilitate their comparison. The final values are in fact very different from each other: for the first excitation $E_I = 0.23\,\text{k Nm}$, $R = 3.3\,\text{k Nm}$ and for the last one $E_I = 24.74\,\text{k Nm}$,

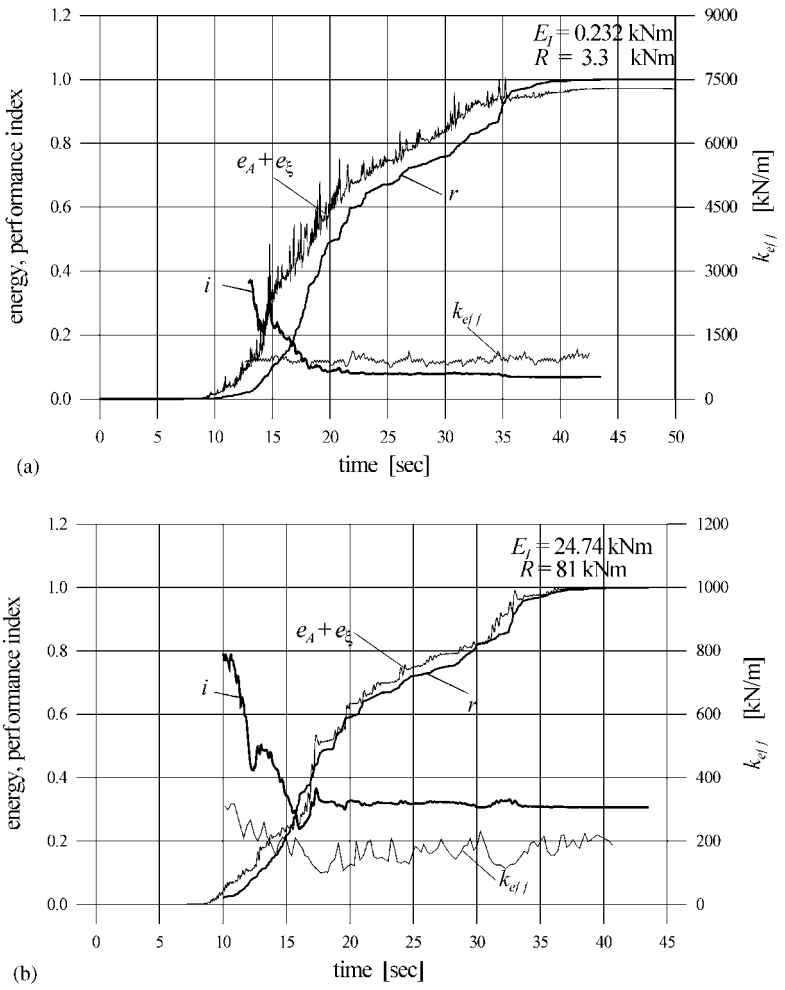

Figure 4. Absorbed and damping energy, referential energy, performance index and effective stiffness of the first mode evaluated from responses in the x-direction during (a) the first shock ($a_M \cong 0.05g$) on building A1, and (b) the last shock ($a_M \cong 0.32g$) on building A1. Energies are normalized to their maximum values.

$R = 81$ k Nm. During the first excitation the building has a basically linear behaviour (with only very modest damage at spandrel beams) with a significant contribution to e_A of the strain energy. Thus, the maximum values of $(e_A + e_\xi)$ occur during the shock, the final input energy E_I being a little lower than it (Figure 4(a)). This feature does not occur when the building is heavily damaged (Figure 4(b)); in these instances maximum values of $(e_A + e_\xi)$ are recorded at the end of the excitation. In both cases $r(t)$ is relatively regular, with only some limited increases (e.g. at $t = 35$ sec for the first test and at $t = 33$ sec for the last one and between 15 and 20 sec for both) which are due to the correspondent increase of base

accelerations. When the system is practically undamaged (Figure 4(a)) the effective stiffness k_{eff} is fairly constant during the response and the function $(e_A + e_\xi)$, although very jagged due to the influence of the strain energy, does not show steep increases in its mean value. On the contrary, during the last base motion, when the building suffers heavy damage, the function $(e_A + e_\xi)$ has some steep increases occurring at $t = 12.8$, 16.4, 19.8, 24 and 32 sec. It may be seen that k_{eff} starts to decrease a little before the beginning of the steep increase of the input energy. The reduction of the stiffness is a signal of the extension of existing damage: the effect is the increase of damping and absorbed hysteretic energy which is reflected on the evolution of $(e_A + e_\xi)$. In correspondence to the time at which k_{eff} starts to show a local decrease, base accelerations become more significant and the referential energy $r(t)$ increases more rapidly than in the previous time intervals: this is made apparent either by an augmented slope of the curve $r(t)$ or by its relatively sharp increase. The increased severity of the base motion affects the amount of the absorbed and damping energy after a delay Δt, of the order of 1–2 sec: it follows that the function $(e_A + e_\xi)$ varies with a minor slope compared to $r(t)$ during Δt. According to the way $i(t)$ is defined, it decreases in Δt, $r(t)$ being in the denominator. In turn, when damage affects the energy dissipation and absorption capacity of the building, $i(t)$ increases following the increase of $(e_A + e_\xi)$. The occurrence of damage is thus characterized by valleys in the function $i(t)$.

The average value of k_{eff} during the last shock on A1 is about 25 per cent the average value determined during the first shock, consistent with the variation of the first mode frequencies reported in Reference [1]. However, it may be observed that the evolution of k_{eff} of Figure 4(b) does not show a decreasing trend over the duration of the response (as occurred in other buildings) but only some local decrease. This is due to the fact that the last shock caused mainly the extension of existing damage, with few new cracks occurring at the beginning of the base motion, during which k_{eff} decreases.

3.3. Qualitative evolution and correlation to damage

The analysis of the evolutions with time of $r(t)$, $(e_A + e_\xi)$, $i(t)$, k_{eff} related to all the damaging shocks acting on the buildings of Table I, pointed out that damage is marked by the items described above: (a) reduction of k_{eff}; (b) concurrent augmented slope of $r(t)$; (c) valleys of $i(t)$ and (d) sharp increases of $(e_A + e_\xi)$, which occurs slightly after the beginning of phase (a). These steps are qualitatively shown in Figure 5; at time t_a, $r(t)$ increases its slope and $i(t)$ starts to decrease. The same happens with k_{eff}. The effect on $(e_A + e_\xi)$ is felt a little later, at time t_b, when $i(t)$ again increases. After t_c a recovery of stiffness occurs and the variation of $(e_A + e_\xi)$ is slower. Valleys of $i(t)$ and steep changes of $(e_A + e_\xi)$ mark the occurrence of damage but do not distinguish its nature (e.g. to spandrel beams or to piers). Damage is, in fact, detected after the shock, and the final value of input energy may be only attributed to variations of the damage pattern with respect to the previous excitations. The only exceptions are when buildings suffer only damage of a given type during the first excitation: in this case it is possible to assess the amount of energy dissipation and adsorption connected to it. As an example, Figure 4(a) shows damage occurring at $t = 14.7$ sec: the detected damage after the shock was a very slight one to spandrel beams; it caused a sudden variation of absorbed energy of about 12 per cent the final one. The important role played by damage to spandrel beams in energy dissipation and absorption capacities of the buildings is confirmed by the analysis of all the cases where it occurred. Further comments on this item will be given in

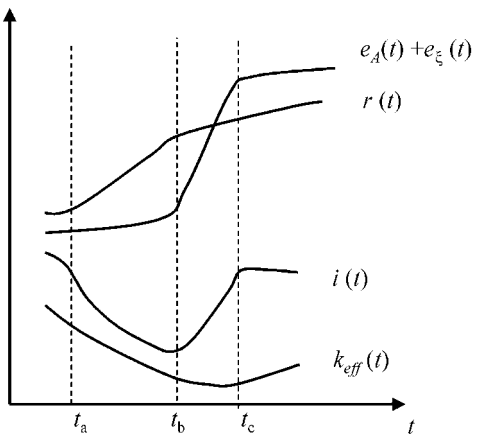

Figure 5. Qualitative evolution of i, e, r and k_{eff} at the occurrence of damage.

the next section. During the first part of the excitations, $i(t)$ tends to decrease with respect to the initial values. For buildings responding basically in a linear way (as in the case of Figure 4(a)) this is due to the predominance of the strain energy on the cumulated damping and absorbed energy. This causes an average slope of $(e_A + e_\xi)$ lower than the corresponding slope of $r(t)$ (see Figure 4(a) in the time interval 15–20 sec).

3.4. Effects of the vertical component of motion

For events causing important damage, the initial decrease of $i(t)$ may be also due to another reason. As an example, consider Figure 6 referred to the last shock on building C1 (before the interrupted one) and to quantities evaluated along the x-direction. C1 is a brick masonry building: it was tested by a series of base inputs of long duration. In the figure energies are normalized to their maximum values. Figure 7 shows the initial portions of the base inputs in the x direction and the vertical one for the said event. Peak accelerations are about $0.26g$ in both cases. The final values of the input and 'referential' energies are, respectively, 17.5 and 105 kN m. During the base motion the structure suffered severe damage at spandrel beams of the two storeys. The evolution of $(e_A + e_\xi)$, of $i(t)$ and of k_{eff} suggests that damage or its extension occurs at times $t = 14$, 17, 21 and 51 sec. (Figure 6). The stiffness decrease starts to appear at $t = 11.8$ sec. Until then, the values of horizontal accelerations are rather low, of the order of $0.04g$ while the vertical excitation is considerably higher, being of the order of up to $0.18g$. Additionally, the Fourier analysis of the two signals shows a richer high-frequencies content for the vertical input than for the horizontal one. The decrease of k_{eff} cannot be attributed to horizontal actions, due to their very low values up to the considered time. A possible interpretation is that the high-frequency components (of relatively high amplitudes) of the vertical signal cause the deterioration of the mechanical properties of the mortar, which is reflected in the decrease of k_{eff}. The subsequent increasing horizontal accelerations act on a structure which has already lost the properties it had at the beginning of the shock and hence produce damage. This feature was observed in all buildings tested in their original

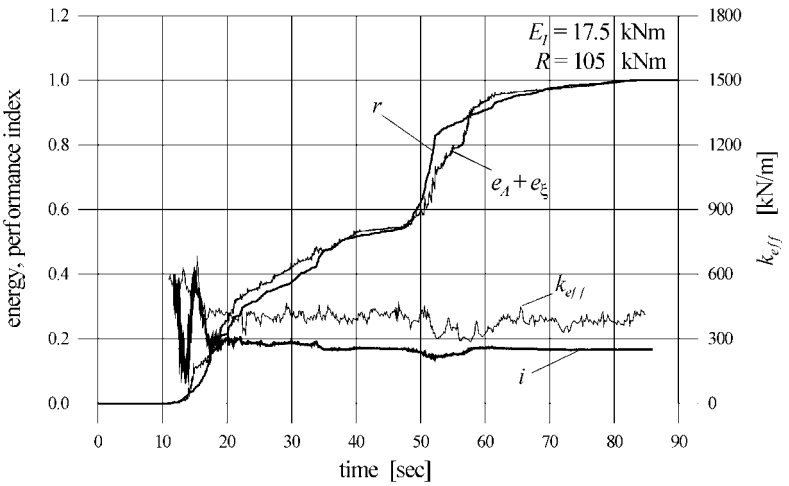

Figure 6. Absorbed and damping energy, referential energy, performance index and effective stiffness of the first mode evaluated from responses in the x-direction during the last shock ($a_M \cong 0.27g$) on building C1. Energies are normalized to their maximum values.

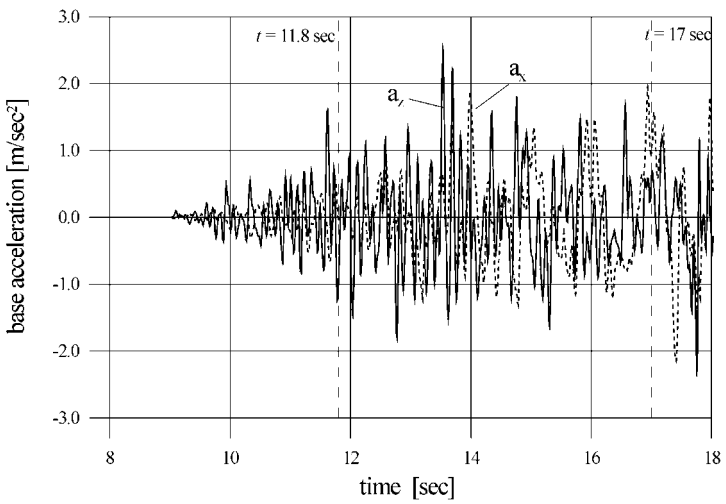

Figure 7. Initial portions of the horizontal (in the x-direction) and vertical acceleration acting on C1 (last test).

configuration, but not in repaired ones. In fact, repairs did not affect the quality and the nature of the mortar, damaged during previous tests. The shaking table tests referred to in this paper gave some hints of the influence of the generally neglected vertical components of motion; this influence deserves further investigation.

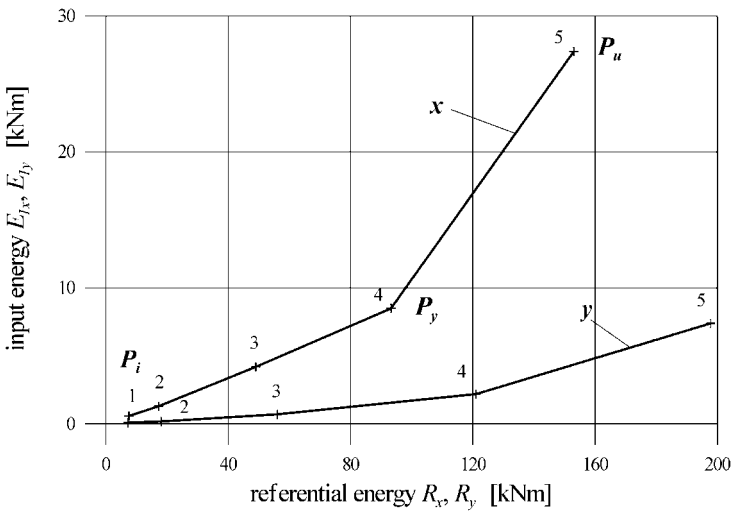

Figure 8. Input energies vs referential energies computed for all the shocks acting on building B1. Numbers 1–5 denote the shocks of the testing sequence.

4. CORRELATION BETWEEN DAMAGE AND TOTAL ENERGIES

4.1. Correlation among E, R and I

The final values of referential and input energies are useful tools in order both to describe the behaviour of a single building during the entire sequence of excitations acting on it and to compare the global behaviour of different buildings. To this aim we can make reference either to quantities evaluated in a given direction (such as E_{Ix}, E_{Iy}, R_x, R_y) or to total quantities (e.g. $E_{It} = E_{Ix} + E_{Iy}$). Since two sets of excitations of different lengths were used (see Table I) and energies involved depend on the duration of the signals, energies pertaining to buildings subjected to longer shocks (B1, B2, C1, C2) were reduced by the ratio of the time length of the shorter shocks (approx. 40 sec) to the one of longer duration (approx. 80 sec). This simple way to reduce energies obtained from the longer shocks is justified by the fact that the short-duration base motions were derived from the long-duration ones in such a way as to have the same frequency content (see Reference [1]). Given its definition, however, the index I is not affected by the above procedure.

As an example of the information that may be derived by the evolution of final input energies during the entire set of excitations acting on a given building, consider Figure 8, which refers to system B1 and to quantities computed along the x and y directions. Input energies E_{Ix} and E_{Iy} are plotted against 'referential' energies R_x and R_y. For the last two shocks, base inputs acting along x and y are rather different; this is reflected in the different values of their R_x and R_y. The figure points out the diversity of the response of the building along the two considered directions, which depends on the different energy absorption and dissipation capacities of x- and y-walls. During the first two shocks no damage was recorded. Some very small cracks were detected at spandrel beams of x-walls after the third test. This

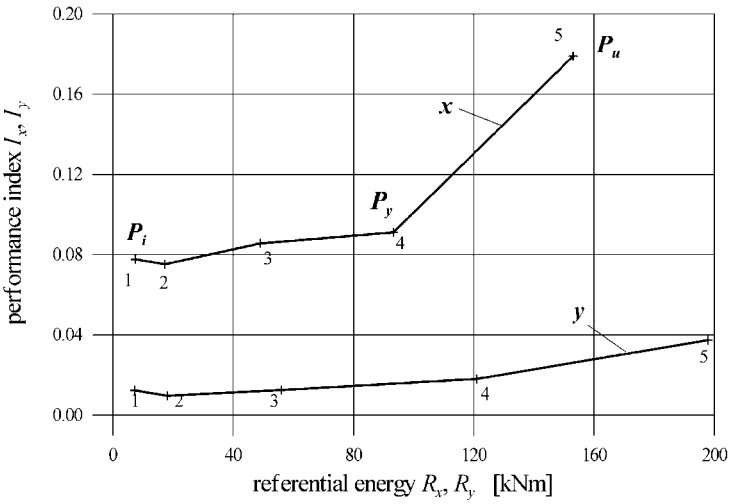

Figure 9. Performance index vs referential energies for building B1.

damage became significant during the fourth and the last excitations; y-walls showed some damage only during the last shock. The evolution of the damage pattern corresponds to the values and to the variations of E_{Ix} and E_{Iy}, E_{Ix} being always considerably greater than E_{Iy} and the slopes of $E_{Ix} - R_x$ curve greater than the ones of $E_{Iy} - R_y$ curve. This fact indicates the significant effect of damage to spandrel beams on energy dissipation and absorption.

The fourth event marks an important change of the response; this is also described by the change of modal parameters occurring after it and reported in Reference [1]. This event, denoted by P_y, may be considered as the one producing the 'significant yield' in the structure; as a matter of fact, lateral force–displacement curves worked out in Reference [1] indicate P_y as the end of the 'linearizable behaviour', in agreement with what is derived from the present energy analysis. It may be noted that the slope of the (E_I, R) curves is fairly constant up to the event P_y. This is reflected in the evolution of the performance indexes I_x and I_y against R_x and R_y, shown in Figure 9. Such indexes are rather constant up to P_y. This feature is recovered for all the tested buildings: significant yield marks the end of the quasi-constant trend of the index. The quasi-constant evolution of I_x and I_y up to P_y is not surprising. In fact, tests have been carried out by scaling base inputs of a factor $\gamma > 1$ with respect to the reference signals. In the ideal case of perfect linear responses the change of both E and R is proportional to γ^2, hence I is approximately constant. The very modest deviations from I approximately constant detected in the tested buildings may be attributed to increases of damping due to slight, and not visible, damage to the mortar. After P_y, when serious damage occurs, important hysteretic effects appear in the structure and E_I increases more rapidly than R, both in the x and y directions, thus producing the change of I. Figure 9 shows that I_x is always higher than I_y, as a consequence of both the larger energy absorption and dissipation capacity of x-walls and the more significant damage suffered by them. The performance index may hence be assumed also to describe the amount of damage to a given structure and its distribution among the main resisting elements (x- and y-walls).

Table II. Values of I at the three phases of behaviour of all the tested buildings.

Model	P_i			P_y			P_u		
	I_x	I_y	I_t	I_x	I_y	I_t	I_x	I_y	I_t
A1	0.069	0.028	0.047	0.123	0.042	0.08	0.305	0.278	0.291
A2	0.09	0.0628	0.075	0.1156	0.0957	0.1045	0.249	0.45	0.38
B1	0.077	0.012	0.045	0.091	0.018	0.049	0.179	0.037	0.099
B2	0.13	0.034	0.079	0.121	0.037	0.080	0.25	0.313	0.282
C1	0.062	0.023	0.041	0.092	0.035	0.061	0.17 (0.42)	0.09 (0.30)	0.12 (0.35)
C2	0.101	0.013	0.054	0.111	0.023	0.065	0.215	0.34	0.274
D1	0.018	0.015	0.017	0.021	0.03	0.025	0.092	0.062	0.076
D2	0.067	0.065	0.066	0.132	0.06	0.091	0.198	0.24	0.22
E1	0.062	0.108	0.087	0.086	0.128	0.108	0.19 (0.44)	0.18 (0.365)	0.19 (0.406)
F1	0.197	0.213	0.206	0.212	0.20	0.20	0.27 (0.388)	0.23 (0.379)	0.24 (0.384)
G1	0.246	0.23	0.236	0.335	0.24	0.284	0.33	0.23	0.25 (0.61)
H1	0.121	0.098	0.109	0.146	0.144	0.145	0.45	0.253	0.345

4.2. Significant phases of behavior

Figures 8 and 9 summarize the 'history' of a given building through the sequence of excitations acting on it; they have been worked out for all the tested systems. Three points are of interest, in that they describe three different phases of behaviour: the first one P_i is related to the basically linear response to the first shock, with peak base inputs of the order of $0.05g$; the second one P_y refers to the significant yield; the third point P_u refers to the response to the last shock. In most instances, particularly for repaired and strengthened systems, the last test caused very severe damage and the corresponding structural behavior may be considered as the ultimate one. For brick masonry buildings, tested in their original configuration (A1, B1, C1, D1), damage produced by the last shock was heavy but not so severe as to consider the structure in its ultimate state; P_u hence denotes situations close to it. For most stone masonry buildings the last test was interrupted to avoid the total collapse, which, however, occurred for system G1.

Table II shows the final values of the 'performance indexes' I_x, I_y, and I_t evaluated at the three considered phases of behaviour P_i, P_y and P_u. Values referred to interrupted tests are between parentheses. The comparison between I_x and I_y gives some information about the different engagement, at P_i, and about the different damage, at P_y and P_u, of x- and y-walls. In most cases x-walls are more engaged (and damaged) than y-walls. Only when an r.c. band is applied at the two storey levels, as happened for building E1 (see Figure 10), is $I_y > I_x$. In these cases, spandrel beams are much stronger and stiffer than in the other configurations and hence reduce the energy dissipation and absorption capacity of x-walls. The values of I_t at P_i are a description of the initial quality of the buildings before the sequence of excitations acting on them. Original BM systems are rather homogeneous, with $I \cong 0.07$; the only exception is D1 which proved to be much better constructed than the other BM systems, showing $I \cong 0.018$.

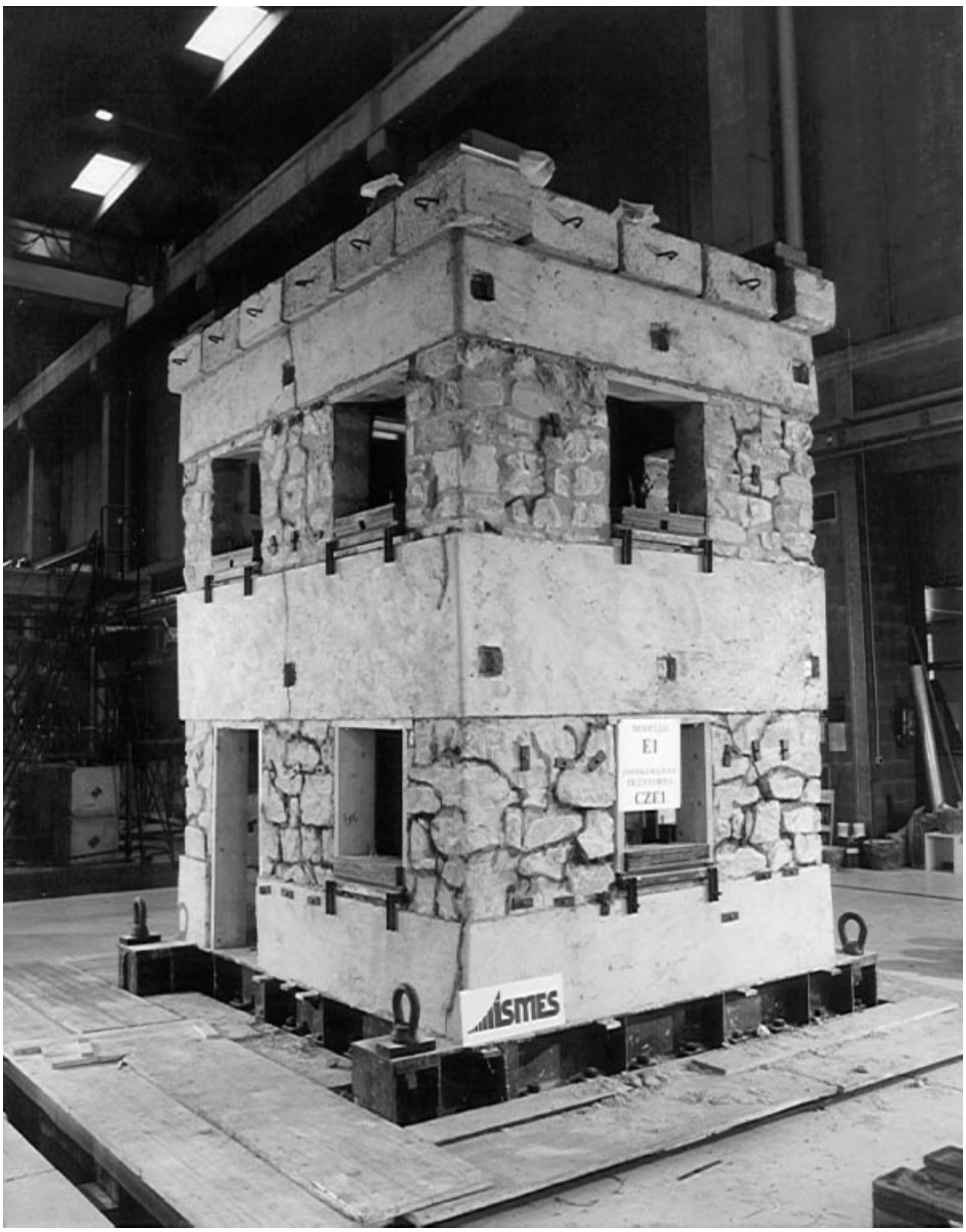

Figure 10. Building E1 strengthened by r.c. bands.

Among SM buildings, G1 and F1 have initially higher indexes than E1 and H1. This is a consequence of the very poor quality of construction for G1, which in fact collapsed during a relatively moderate shock, and of damage caused on F1 during the transportation to the shaking table. It may be noted that the index is able to account for these mishaps and might

be used for diagnostic purposes of real buildings, provided responses, even to very low base inputs, are available.

Each building was subjected to several tests, that caused progressive increase of damage and decrease of modal frequencies: e.g. at the end of testing sequences the first mode frequencies were 30–50 per cent the initial values (see Reference [1]). It is of interest to correlate the change of frequencies to the variation of input energies. In order to be independent of the increase of the severity of base motions during the testing sequence, it is convenient to refer to the normalized input energies, i.e. to I. The variations ΔI of the index and Δf of the first mode frequencies, along the x and y directions, occurring between P_i and P_y and between P_y and P_u have been evaluated for all the systems together with the relevant ratios $\rho = \Delta I/\Delta f$. It was found that ρ values determined for each system, respectively, between P_i and P_y and between P_y and P_u, are fairly similar: for instance, for buildings A1, A2, D2, E1 ρ (in the x direction) is 0.098 and 0.085 (for A1), 0.046 and 0.045 (for A2), 0.051 and 0.033 (for D2), 0.043 and 0.037 (for E1). Although space limitations prevent a detailed presentation and discussion of these results, it may be seen that frequencies and normalized input energies vary roughly in a similar way during the sequence of excitations acting on a given building, both quantities depending on the evolution of damage.

4.3. Effects of retrofittings on I_t and E_{It}

It may be seen from Table II that for the original BM buildings $I_x > I_y$ at all three considered phases of behaviour, while after repairs this was the case only up to the significant yield P_y, being at ultimate $I_x \leqslant I_y$. These facts may be explained by considering that repaired BM buildings were subjected to final shocks that were considerably more severe than those acting on the original configurations, hence their behaviour may be properly considered as the ultimate one. Additionally, all repairs and strengthenings were aimed at connecting all the walls of the building (see Table I) by means of horizontal tendons or internal and external r.c. bands. These proved able to fully engage, during the final response, both x- and y-walls, as a consequence of a 'compact' box-type response mechanism. The same holds for the two SM buildings E1 and F1 strengthened in a similar way. It turns out that those interventions enforce a more homogeneous global behaviour at ultimate of buildings than the other considered ones.

Figures 11, 12 and 13 show E_{It} as a function of R_t for all the tests carried out, respectively, on BM buildings in their original (Figure 11) and repaired (Figure 12) configurations and on SM systems (Figure 13); in these figures the points referred to the phases P_i, P_y and P_u are denoted by different symbols. It may be seen again that buildings subjected to prior (SM) or repair (BM) interventions show a reduced scatter with respect to BM original systems, thus supporting the above comments about the effect of repairs and strengthenings. Maximum values of R_t and E_{It} occur for repaired BM buildings: they are, respectively, 7 and 6.5 times higher than the corresponding largest values of SM buildings due to the larger base excitations needed to cause ultimate conditions on strengthened BM systems. During the initial phase of behaviour and up to P_y, repaired BM buildings engage energy dissipation capacities higher than those of the corresponding original systems: this may be seen from the values of I_t at P_i and P_y reported in Table II. Up to the significant yield the input energy is mainly due to non-hysteretic phenomena, damage being still limited. Table II shows that, for SM buildings, the values of the total 'performance' index at P_y are higher (up to 4 times) than the ones occurring at P_y for both the original and repaired SM systems, thus showing that stone masonry dissipates

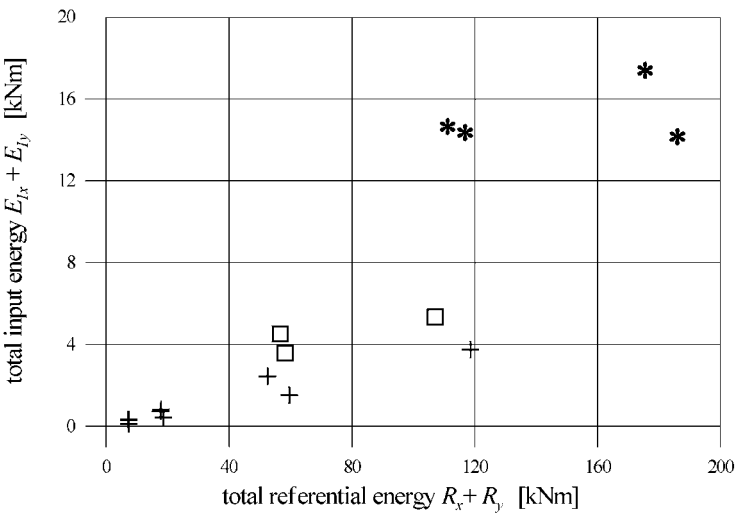

Figure 11. Input energy vs referential energy for original BM systems. Symbols (□) and (∗) refer, respectively, to the significant yield and to the ultimate state.

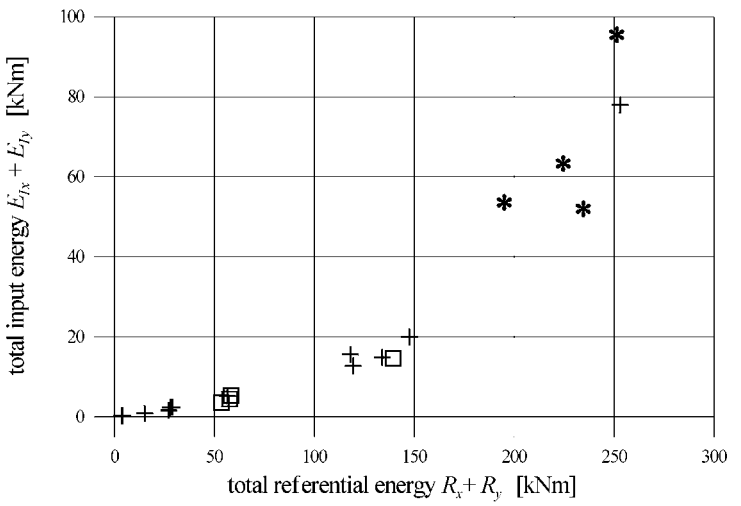

Figure 12. Input energy vs referential energy for repaired BM systems. Symbols (□) and (∗) refer, respectively, to the significant yield and to the ultimate state.

significantly more than brick masonry. This result is consistent with the values of damping identified in Reference [1] for SM and BM up to P_y.

However, during very severe excitations, engaging buildings to their true ultimate states and causing heavy damage, I_t values for SM systems and for strengthened BM ones are very similar (of the order of 0.35), although the total absorbed and damping energies E_{It} are higher for strengthened BM buildings than for SM ones, due to the higher severity of base inputs

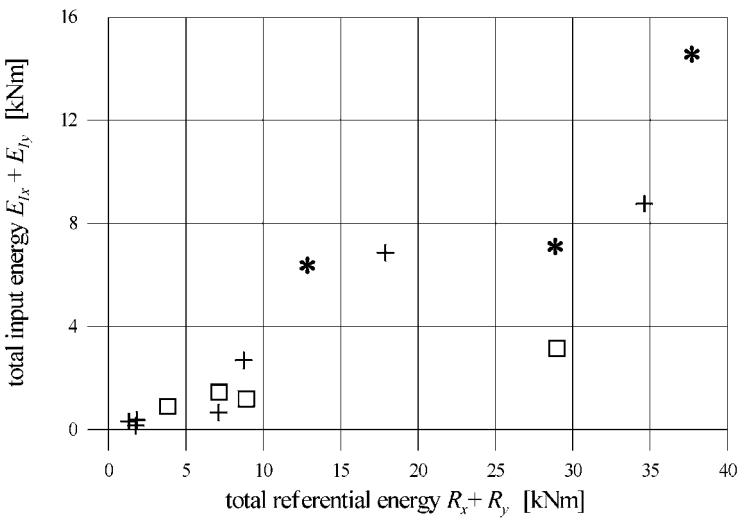

Figure 13. Input energy vs referential energy for SM systems. Symbols (□) and (∗) refer, respectively, to the significant yield and to the ultimate state.

involved in the final responses of repaired BM structures. This fact shows that the hysteretic behaviour occurring at ultimate state is similar in the two types of buildings, and is independent of the material employed for construction.

If 'anomalous' buildings (D1, F1 and G1) are excluded (D1 was of much better quality than the other BM systems, F1 was damaged during the transportation to the shaking table and G1 was very poorly built, with practically no connections between orthogonal walls), Table II shows that at significant yield I_t is around 0.06–0.1 for BM systems and 0.1–0.15 for SM ones; at ultimate I_t is about 0.30–0.35 for BM (if only true ultimate conditions are taken into account) and about 0.34–0.38 for SM buildings. The above values roughly characterize different phases of behaviour of masonry buildings: their possible use is the tentative assessment of 'how far' from ultimate or yielding conditions is a given building for which base and response signals are available. This rough assessment may be provided by the comparison of its actual I to the values of the performance index at P_y and at P_u, evaluated for the considered type of building.

4.4. Preferable damage states

After each excitation buildings have been surveyed in order to assess the evolution of the damage pattern. The type of damage (new or extension of existing damage) recorded between two shocks was correlated to the relevant variations ΔR and ΔE_{I} of referential and input energies. A detailed description of these correlations is not given here due to space limitations. We only draw attention to one of the most important phenomena that have been observed and previously mentioned: the effect of damage to spandrel beams on energy absorption. To this aim consider first Figure 14 where $E_{\mathrm{I}x}$ is plotted against R_x for all the shocks acting on building A2. This structure was repaired by the application of r.c. bands at each level, similar to E1: their effect

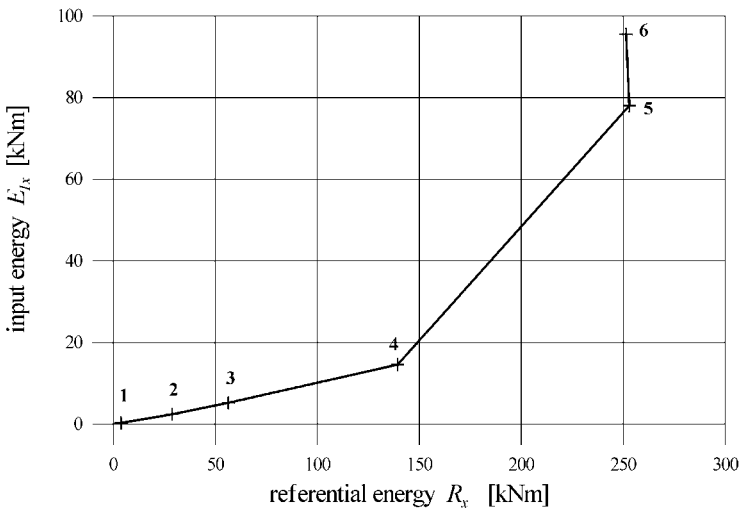

Figure 14. Input and referential energies in the x-direction for building A2.

was to efficiently tie together the building and to significantly strengthen spandrel beams, which in fact did not suffer important damage until the very last excitation, during which important damage was recorded at spandrel beams. The last base motion was practically identical to the previous one, as shown by the very similar values of R_{5x} and R_{6x}. Correspondingly, input energies between tests 5 and 6 vary by about 30 per cent. The variation of damage between the two tests consists mainly in very serious cracks appearing at spandrel beams in x-walls. It turns out that the increase of input energy has to be attributed to damage to spandrel beams. In order to make this point clearer it is convenient to introduce the following indexes:

$$\alpha_R = \frac{\Delta R}{R_1}, \qquad \alpha_E = \frac{\Delta E_1}{E_1}, \qquad \alpha = \frac{\alpha_E}{\alpha_R}$$

ΔR and ΔE_1 being the increments of referential and input energies in a given direction occurring between two subsequent shocks and R_1 and E_1 the energies related to the first of the two considered excitations. In the case of perfectly linear behaviour $\alpha = 1$; when $\alpha > 1$ the greater the value of α, the greater non-linear behaviour occurs, with energy absorption and dissipation capacity increasing more than the base referential energy. In some buildings, damage occurred during the last two shocks only at spandrel beams, predominantly of x-walls. This happened for buildings B1, C1, D1. On the other hand, for building E1, which was strengthened by using r.c. bands at each level, damage was concentrated at piers, with only some small cracks at spandrel beams. By computing α with reference to the x-direction and to the last two shocks, the following values were obtained: $\alpha = 3.45$, 3.98, 5.16 for B1, C1 and D1; $\alpha = 2.57$ for E1. For E1 the same value of α is also found if the third and fourth shocks are considered, when important damage occurs first at piers. The above values quantify the greater influence on energy absorption and dissipation due to damage to spandrel beams with respect to that to piers. For the same increments of referential energy, which is a description of the severity of the shock, damage to spandrel beams involves increments of input energy that are 40–100

per cent higher than those related to pier cracking. This result may influence the choice of the repair/strengthening interventions on masonry buildings, promoting the study of devices that allow highly energy-consuming damage to spandrel beams, although controlling it. This type of damage is more preferable than damage to piers: their collapse determines, in fact, the collapse of the entire structure.

5. CONCLUSIONS

Energy functions have been evaluated from the responses to the 58 base excitations acting on the 12 stone and brick masonry buildings. The severity of each shock is described by $r(t)$, depending on the considered ground motion, while the behaviour of the building during the excitation is described by the 'performance index' $i(t)$, the ratio to $r(t)$ of the input energy $e_I(t)$. The function $i(t)$ was found to be a good descriptor of the behaviour of the structure: when the structure responds linearly, $i(t)$ is basically constant; valleys in $i(t)$ correspond to sharp increases of $e(t)$ and denote the occurrence or the extension of damage. The variations of the performance index with time are consistent with the variations of modal parameters of the dominant mode during the response, as was mentioned. The analysis of the above functions enables to detect the occurrence of damage during the response and may be seen as a method, based on energy functions, for the interpretation of seismic responses. Its application provided some hints for assessing the effect of the vertical component of ground motion on structural behaviour.

The comparison of R, I and E_I (the values of the above functions at the end of the excitation) pertaining to the considered shocks and buildings allows a quantitative description of the energy dissipation and absorption capacities connected with the different materials of the buildings, with their state of damage and with the different strengthenings considered. Of particular interest is the influence of damage to spandrel beams on the energy absorption capacity, which is much higher than that determined by other types of damage. This fact may result in a strengthening strategy aimed at allowing this damage to occur, while controlling it, in order to protect the structure from collapse. This possible strengthening method may be considered as new for the type of buildings herein taken into account, but needs further analysis.

REFERENCES

1. Benedetti D, Carydis P, Pezzoli P. Shaking table tests on 24 masonry buildings. *Earthquake Engineering and Structural Dynamics* 1998; **27**:67–90.
2. Uang CM, Bertero VV. Evaluation of seismic energy in structures. *Earthquake Engineering and Structural Dynamics* 1990; **19**:77–90.

